INSTITUTE OF PHYSICS PUBLISHING NANOTECHNOLOGY

Nanotechnology **17** (2006) 5271–5277 doi:10.1088/0957-4484/17/20/038

Large scale synthesis of CdS nanorods and its utilization in photo-catalytic H_2 production

C M Janet and R P Viswanath[1]

Department of Chemistry, Indian Institute of Technology Madras, Chennai-600036, India

E-mail: rpv@iitm.ac.in

Received 30 June 2006, in final form 15 September 2006
Published 3 October 2006
Online at stacks.iop.org/Nano/17/5271

Abstract
CdS nanorods along with nanostrips and plates have been prepared on a large scale by the solvothermal route using the precursor cadmium oxalate under mild conditions with ethylene glycol as the solvent and $(NH_4)_2S$ as the sulfiding agent, without using catalysts, surfactants or template. The aspect ratio of the rods varied from 3 to 30. Characterization has been done by TEM, HR-TEM, EDX, HR-SEM, XRD, BET surface area, UV–vis absorption, photoluminescence and fluorescence studies. Photo-catalytic H_2 production activity was tested with as-synthesized CdS, calcined CdS, noble metal loaded CdS and for bulk CdS. The nanorods being formed are used as such for H_2 production. The as-synthesized CdS is found to have very good H_2 production capacity compared to that of the bulk CdS. Upon Pt loading much enhanced activity was observed in the rate of hydrogen production.

(Some figures in this article are in colour only in the electronic version)

M Supplementary data files are available from stacks.iop.org/Nano/17/5271

1. Introduction

Nanoscale one-dimensional structures have attracted considerable attention due to their unique electronic, optical, catalytic and mechanical properties. The development of synthesis methods, control of morphology, and assembly of desired nanostructures still remains a challenge in this field. Due to the shape selectivity of the properties, synthesis of one-dimensional semiconductor materials such as nanowires, nanorods, nanofibres or nanoplates has been the focus of research work [1–3]. Recently, various methods have been used for the preparation of nanorods or nanowires, such as solution–liquid–solid growth, laser ablation, carbon-nanotube-confined reaction, electrochemical fabrication and non-aqueous solution synthesis [4–9]. In the nano regime most of the compounds show much enhanced activity compared with the bulk sample due to their increased surface area and the suitable orientation of the catalytically active planes.

Chalcogenides have been reported as active photo-catalysts for the reduction of H_2O to H_2 [10]. By taking into consideration the present interest in the field of hydrogen production from cheaply available sources, CdS has been utilized for the H_2 production from photo-catalytic water splitting. Photo-catalysis has potential application for the conversion of solar energy into chemical energy and for the treatment of pollution [11–14]. Bulk CdS absorbs visible light because of its narrow bandgap (2.4 eV) [14–16]. In addition, its sufficiently negative flat band position [-0.66 V at pH 7] is suitable for the photo-generated electrons to carry out the reduction of H_2O to H_2. The essential steps of the reaction include the separation of electrons and holes by absorption of light by CdS and the transfer of electrons to its conduction band. Absorption of light by a photo-catalyst increases by increasing the surface area of CdS per unit volume of catalyst. Surface area and bandgap can be increased when the particle size reduces to nano dimensions. Increase in bandgap shifts the absorption from the visible to the UV region. However, in nanostructures, recombination of photo-generated electrons and holes also takes place at an enhanced rate due to inadequate bending of bands. Thus, considerable attention has been paid to prevent charge recombination in order to improve the

---

[1] Author to whom any correspondence should be addressed.

0957-4484/06/205271+07$30.00

activity of CdS. The step reported in the literature to prevent charge recombination is by doping with metals like Pt to the semiconductor so that the photo-generated electrons are transferred from the conduction band of CdS to the Pt metal. Incorporation of another semiconductor has also been reported to improve the activity [17]. In this paper we report the synthesis of CdS nanorods via the solvothermal route using a novel precursor and these nanorods have been effectively used for the photocatalytic H_2 production.

2. Experimental section

2.1. Materials and methods

Preparation of CdS nanostructures involved an initial synthesis of cadmium precursor cadmium oxalate from 1 M each of $Cd(NO_3)_2 \cdot 4H_2O$ and $K_2C_2O_4 \cdot H_2O$. Cadmium oxalate formed was filtered, washed with deionized water and dried in a hot air oven at 120 °C. Formation of cadmium oxalate was confirmed by XRD. About 1 g of cadmium oxalate was weighed and transferred to a two neck round bottom flask. Ethylene glycol (20 ml) was added to this and stirred well until a good dispersion was achieved. Ammonium sulfide (20%, 10 ml) was then added to the mixture slowly and refluxed in a stream of Ar atmosphere in an oil bath, which was maintained at a temperature of 60 °C for 3 h. An excess of $(NH_4)_2S$ had been taken to facilitate the complete conversion of oxalate to sulfide. The yellow CdS formed was filtered and washed with absolute ethanol and dried in a hot air oven at 150 °C. In order to study the effect of calcination CdS as synthesized was calcined first in air atmosphere for 30 min to remove the organic impurities and then for 3 h in N_2 atmosphere at a temperature of 350 °C. Pt (1%, 0.2%) loading of CdS was done by the impregnation method using H_2PtCl_6 solution. Bulk CdS has been prepared by the simple addition of 1 M solutions of $CdNO_3 \cdot 4H_2O$ and $(NH_4)_2S$. The orange coloured precipitate obtained was filtered, washed with deionized water and dried in an oven at 120 °C. All the five samples were tested for their photo-catalytic activity under UV light towards H_2 production.

2.2. Characterization

Characterization has been done using TEM, EDX, HR-SEM, XRD, UV–visible spectra, photoluminescence and fluorescence studies. Surface area was determined by the BET N_2 adsorption method. Powder x-ray diffraction patterns of the CdS samples were recorded using a Shimadzu XD-D1 diffractometer using Ni-filtered Cu Kα radiation ($\lambda = 1.5418$ Å). UV–visible absorption spectra were recorded using a Varian Cary 5E UV–vis–NIR spectrophotometer in the spectral range of 200–800 nm. Absorption spectra for catalyst samples were recorded as Nujol paste. The specific surface area, pore size and pore volume of the samples were measured using a Sorptomatic 1990 instrument at 77 K. Prior to the sorptometric experiment, the samples were degassed at 150 °C for 12 h. The surface morphology of the CdS particles was analysed using SEM images using a JSM-6330F, high resolution scanning electron microscope (HR-SEM) operating at 20 kV. The transmission electron micrographs (TEMs) were recorded with a JEOL-JEM 100SX microscope, working at a 100 kV accelerating voltage. High resolution transmission electron microscopy (HRTEM) was performed using a JEOL-3010 transmission electron microscope operating at 300 kV. Samples for TEM were prepared by dispersing the powdered sample in ethanol by sonication and then drip drying on a copper grid (400 mesh) coated with carbon film. Photoluminescence (PL) measurements were carried out on a Hitachi 850-type visible ultraviolet spectrophotometer with a Xe lamp as the excitation light source and the fluorescence measurements were made on a Hitachi F-4500 spectrofluorimeter with an Xe lamp of voltage 100 W. Gas chromatographic analysis was done on a Nucon model 5765 gas chromatograph.

2.3. Photo-catalytic study

About 0.1 g of the catalyst sample was weighed and transferred to a quartz reactor containing 50 ml of an aqueous solution of both 0.35 M Na_2S and 0.24 M Na_2SO_3 with a pH of 9.7 ± 0.1. The mixture, S^{2-}/SO_3^{2-}, is acting as the sacrificial agent here [18]. Further improvement of the hydrogen evolution could be achieved by loading the Pt on the CdS. Chemical interaction between CdS and another semiconductor or metal will affect the low energy surface states of CdS, leading to an enhanced activity. Photo-catalytic hydrogen evolution experiments were performed on these materials using a quartz reactor with options for water circulation at the outer wall of the reactor and specific outlet for gas collection. Before illumination by a UV source, the solution was de-aerated with nitrogen gas for 30 min to remove the dissolved oxygen. Then the mixture was irradiated with a 400 W Hg lamp (Oriel Corporation, USA). The lamp has a wavelength distribution ranging from 200 to 2500 nm (including UV–visible and near IR) with a peak wavelength of 365 nm. The evolved gas was collected over brine water using an inverted gas burette.

The gaseous products, after being collected, were analysed using an FFAP column and thermal conductivity detector (TCD) for the confirmation of H_2. For the detection of hydrogen, nitrogen was used as the carrier gas and for that of oxygen/moisture the carrier gas was hydrogen. Traces of moisture and oxygen have been detected using SE-30 as the column. Moisture may be coming from the aqueous reaction medium, along with the liberated gas.

3. Results and discussion

3.1. X-ray diffraction studies

X-ray diffraction patterns of the various samples are given in figure 1. Analysis of the diffractogram indicated CdS nanorods (pattern A) to be a mixture of two phases, namely, hexagonal and cubic (JCPDS file No 800006 and 890440). Considerable broadening is evident from the XRD data. It has been observed that one particular plane, hexagonal (100), has preferentially grown [19] as the maximum intense peak, whereas the other two planes (002) and (101) have diminished intensities. This is an indication of one dimensional growth of the CdS. In the case of the calcined sample (pattern B) at 350 °C one can see more crystalline and clear CdS peaks of only hexagonal phase, and pattern C shows the highly amorphous nature of the bulk CdS. The (1%) Pt loaded sample (pattern D) shows much diminished CdS peaks along with a well defined peak of crystalline Pt. The

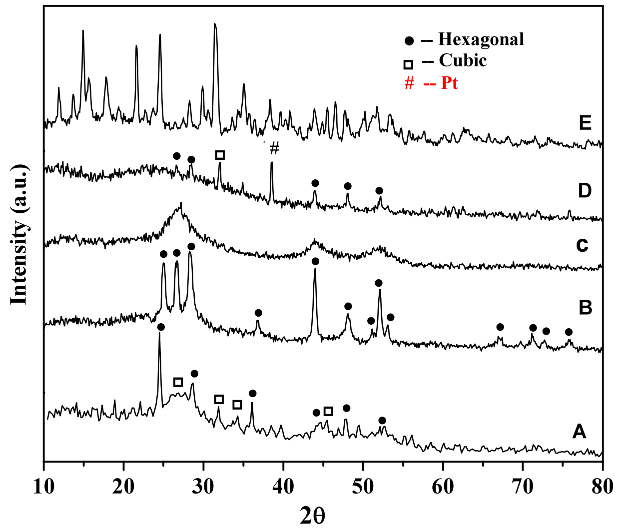

Figure 1. X-ray diffractogram of (A) CdS nanorods as synthesized; (B) calcined CdS; (C) bulk CdS; (D) Pt/CdS and (E) cadmium oxalate.

XRD pattern of cadmium oxalate (pattern E) matches with that of its JCPDS file No 140712, and it can be seen that there are no cadmium oxalate peaks present in the as-synthesized sample. The crystallite size of the as-synthesized CdS nanostructures has been calculated using the Scherrer equation [20] from FWHM values of the peak corresponding to the cubic (200) with a $2\theta = 30.6$ and is around 6 nm. The size calculated for the hexagonal (102) plane at $2\theta = 36$ is around 21 nm, which conveys that the hexagonal CdS has bigger particle size. These particle size values calculated from XRD using the Scherrer equation match with that of the actual width of the nanorods calculated from the TEM images (figure 2).

3.2. *Transmission electron microscopic studies*

TEM images are given in figure 2. From the TEM pictures it is calculated that the length and the width of the rods and plates vary in the range 90–200 nm and 6–20 nm respectively. The single crystalline nature is evident from the electron diffraction pattern. The energy dispersive x-ray analysis (EDX) spectrum (figure 3) shows the presence of cadmium and sulfur. In the case of the calcined sample (figure 4), an increase in size is observed in the TEM pictures. This increase in size explains the lesser activity observed upon calcination for photo-catalytic water splitting. Calcination will enhance the agglomeration of the nanorods to form bigger particles, thus reducing the surface area. Calcined CdS is found to have a size distribution of 160–250 nm. The ring pattern of the electron diffractogram obtained for the calcined sample is proving its polycrystalline nature. The lattice spacing (figure 5) calculated from the HR-TEM exactly matches that calculated from XRD and is equal to 3.32 Å, which is in good agreement

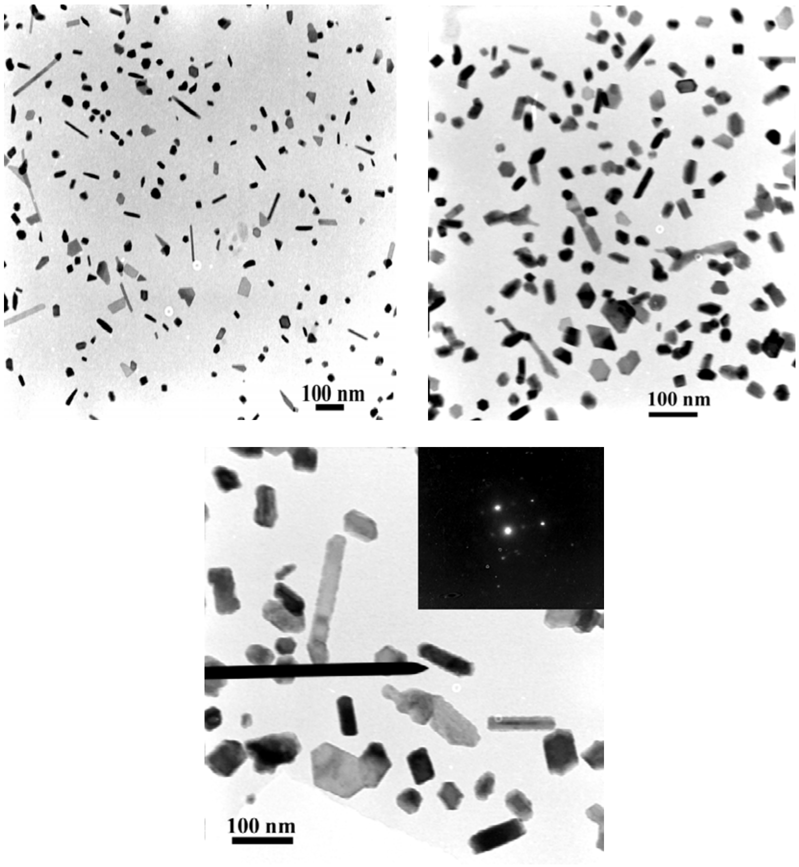

Figure 2. TEM pictures of the CdS nanostructures as synthesized. The SAED pattern for CdS as synthesized is shown in the inset.

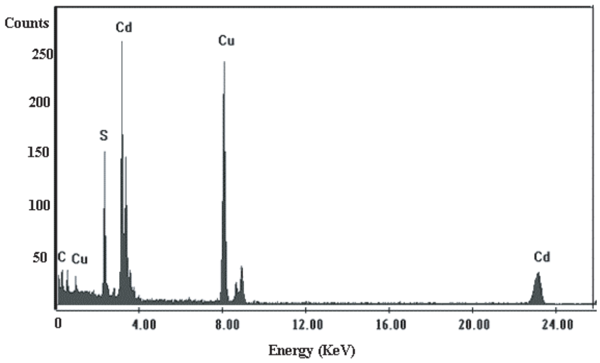

Figure 3. EDX spectrum obtained from CdS nanorods.

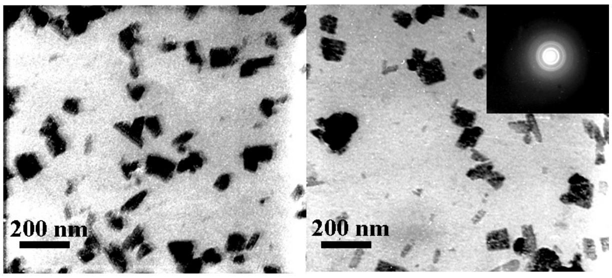

Figure 4. TEM of CdS nanorods after calcination at 350 °C; SAED pattern shown in the inset.

Table 1. Bandgap values of the samples calculated from the UV–visible absorption spectra.

Sample name	Onset of absorption (nm)	Bandgap (eV)
CdS nanorods	483	2.57
CdS nanorods calcined	512.4	2.42
CdS bulk	531	2.34

with the JCPDS d spacing value for the (111) plane of the cubic phase of CdS. Supplementary data files are available at stacks.iop.org/Nano/17/5271

3.3. Optical absorption studies

UV–visible absorption spectra were recorded for CdS nanorods as synthesized, CdS nanorods calcined and for the bulk CdS (figure 6). The onset of absorption in the as-synthesized CdS nanorods is at 483 nm. In the calcined sample and in the bulk CdS the onset of absorption is 512.4 and 531 nm respectively. CdS is a typical direct bandgap semiconductor. When the size of CdS nanocrystals becomes smaller than the exciton radius, a remarkable quantum size effect leads to a size-dependent increase in the bandgap and a blue-shift in the absorption onset [21]. The increment in bandgap is approximately inversely proportional to the square of the crystal size based on the effective mass approximation [22]. The bandgap of CdS is affected by the preparation technique; but no consistent correlation seems to exist between the bandgap and the activity. The values of bandgap calculated [23] for the three samples are given in table 1.

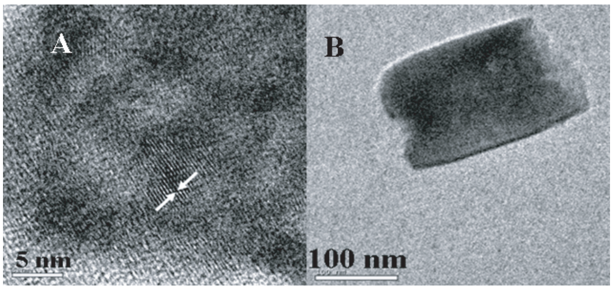

Figure 5. HR-TEM images of CdS nanorods: (A) CdS lattice; (B) CdS nanoplate.

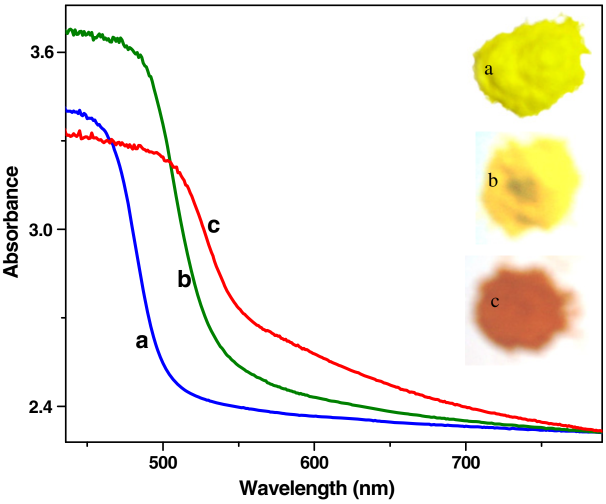

Figure 6. UV–visible absorbance spectra of (a) CdS nanorods; (b) calcined CdS nanorods and (c) bulk CdS.

3.4. Photo-luminescence spectroscopy

Photoluminescence (PL) measurements were carried out at room temperature with excitation wavelength 483 nm. Photoluminescence spectra of the solid sample of the CdS nanorods are shown in figure 7. As expected we have two emission peaks, corresponding to exciton emission (533 nm), which is sharp and located near the absorption edge, and the second one, which is located at a longer wavelength (668 nm), which is broad and due to the trapped states [24] present because of the surface excess of either Cd^{2+} or S^{2-} ions. When we excited the sample at 238 nm (figure 8), where there was one weak absorption, we could get a very weak low intensity emission at 346 nm, which can be attributed to a higher level transition in the CdS crystallites. Reports are available that this kind of band edge luminescence is caused by the recombination of excitons or shallowly trapped electron–hole pairs. The apparent blue-shift and the strong peaks are also indicative of the size quantization of as-prepared CdS nanorods.

3.5. Fluorescence spectroscopy

The spectra are typically asymmetric (figure 9) and suggest strong acoustic phonon coupling but weakly intense in the case of CdS. Fluorescence emission from the CdS nanorods

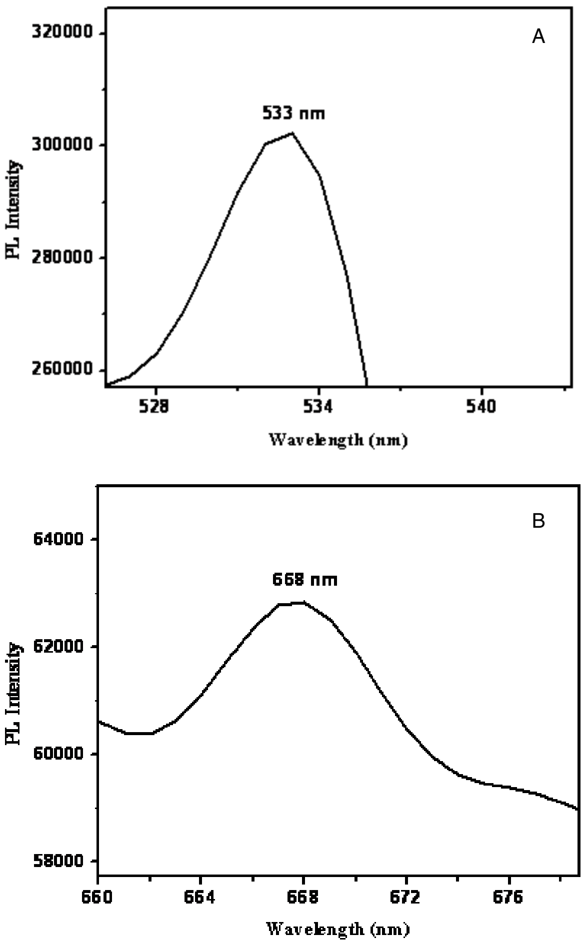

Figure 7. Photoluminescence spectra of the CdS nanorods at room temperature; the excitation wavelength for the emission spectra is 483 nm. (A) Emission due to the excitons and (B) emission due to the trapped states or excess surface states.

is broad, probably indicating a distribution of particle sizes or shapes, and the same is corroborated by the TEM pictures.

3.6. *High resolution scanning electron microscopic measurements*

HR-SEM images are given in figure 10. It is evident from the image that the as-prepared sample has a dendritic [25] surface morphology and each leaf-like projection forming the dendritic structure has many crests and troughs, which increases the surface area. This explains the increased catalytic activity of the as-synthesized sample. Calcined sample surface morphology reveals the complete destruction of the active sites due to agglomeration and hence poor activity.

3.7. *Surface area and pore volume analysis*

CdS nanostructures as synthesized are found to have the highest surface area and pore volume and hence activity also. Calcined CdS is found to have better surface area and pore volume values (table 2) when compared to bulk CdS, even though the catalytic activity was found to be almost the same. This may be due to the partial destruction of the active sites upon calcination.

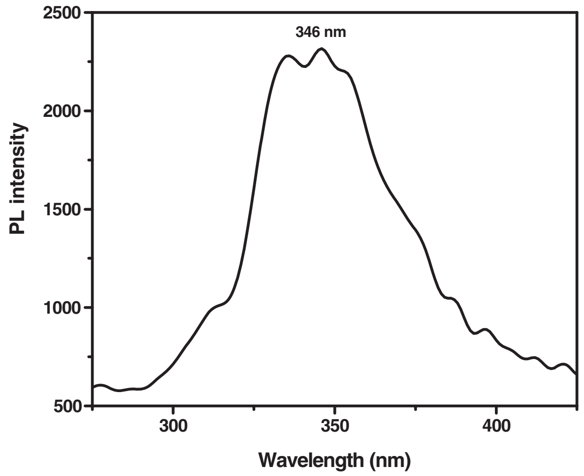

Figure 8. Photoluminescence spectrum; excitation wavelength 238 nm.

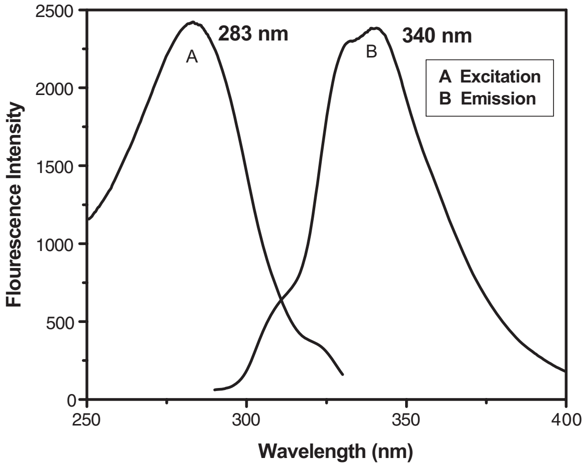

Figure 9. Fluorescence spectrum of the sample: CdS nanorods emit white light at 340 nm under photo-luminescent excitation at 283 nm.

3.8. *Mechanism of nanostructure formation*

Various nanostructure formations can be explained by the following proposed mechanism. Cadmium oxalate has a three-dimensional network structure with oxalate as the binding ligand. When ammonium sulfide is added to such a system the excess Cd^{2+} ions on the surface will react with sulfide ions (scheme 1), thus initiating the sulfide formation. Replacement of the oxalate ligand is from the surface and only one side of the material is exposed to sulfur, which means there will be the formation of nanorods because of the one dimensional growth, and if the oxalate ligands are replaced simultaneously from each side then there will be a planar growth of the CdS leading to the plates and strips. Similarly, the growth as well as the replacement can take place in oriented planes, leading to various polygonal structures.

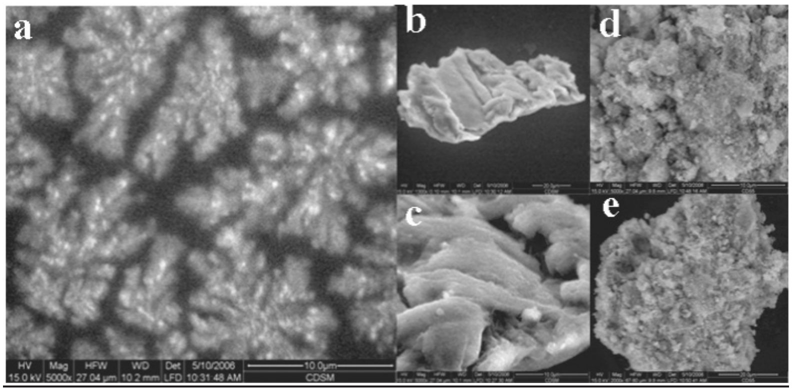

Figure 10. HR-SEM images of (a) as-prepared CdS (dendritic surface morphology); (b) one leaf-like projection of the dendritic structure; (c) crests and troughs on the surface; (d), (e) surface morphology of the CdS nanorods calcined at 350 °C.

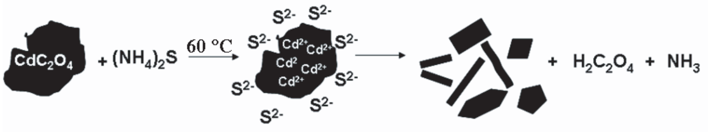

Scheme 1. A proposed mechanism for the growth of CdS nanostructures in ethylene glycol medium.

Table 2. Specific surface areas and pore volumes of the CdS samples.

Sample name	BET surface area ($m^2\ g^{-1}$)	Pore volume ($cm^3\ g^{-1}$)
CdS nanorods	43.09	0.1539
Calcined CdS	12.50	0.0505
Bulk CdS	4.61	0.0241

3.9. Photo-catalytic activity

The photo-catalytic studies for hydrogen production have been conducted with CdS particles suspended in a solution containing a mixture of S^{2-}/SO_3^{2-} species. Here this mixture acts as a sacrificial agent [18]. Addition of sulfite ions, which efficiently suppresses the formation of elemental sulfur, allowed hydrogen to evolve at a higher rate. As a hole scavenger, Na_2S is superior to Na_2SO_3 with respect to increasing the hydrogen evolution. The sustained activity was observed for the CdS samples during the course of the reaction. This can be attributed to the regeneration of sulfide ions in the presence of sulphite, thus preventing the photo-corrosion of the CdS catalyst [26]. The corresponding chemical equations are given:

$$S + S^{2-} \rightarrow S_2^{2-}$$

$$S_2^{2-} + SO_3^{2-} \rightarrow S_2O_3^{2-} + S^{2-}.$$

Further improvement of the hydrogen evolution could be achieved by loading the Pt on the CdS. Chemical interaction between CdS and another semiconductor or metal will affect the low energy surface states of CdS, leading to an enhanced activity. Hence, under the given experimental conditions, the presence of sacrificial agent, an electron sink in the form of Pt on the surface and the morphology of the particle have perceptible influence on the photo-catalytic hydrogen production.

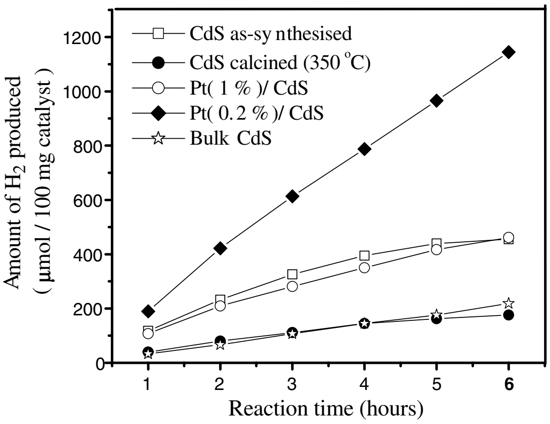

Figure 11. The amount of hydrogen produced on various catalysts.

In photo-catalytic hydrogen evolution activity, the 0.2% Pt loaded sample is found to give the highest activity among all other catalyst systems tested (figure 11). Almost 26 ml of H_2 is produced after 6 h of the light exposure. Moreover, it is observed that the CdS nanorod as synthesized gives a better activity than even the 1% Pt loaded CdS nanorod. This is because of the partial covering of the CdS surface by Pt and hence the light interaction with the surface will be minimized. Thus if the amount of Pt is more on the surface, the photo-activity will be less. Apart from this, as-synthesized CdS has a mixture of hexagonal and cubic phases, out of which the cubic phase is more photo-active [27] for the H_2 production. Calcined and bulk samples are found to give almost the same activity. The calcined sample is crystalline with a definite band structure and phase structure (hexagonal) and the bulk sample is amorphous with no defined bandgap. Even then the activities are quite similar. From this one can say only qualitatively that the cubic phase is more photoactive than the other forms of CdS. Apart from the size effect, there are other parameters on which the photo-absorption depends and hence no generalization can be made with phase structure and photocatalytic activity.

4. Conclusions

We have described a simple chemical method to directly prepare CdS nanostructures without any catalysts, surfactants or template. The reaction conditions are simple and can also be done under atmospheric bench top conditions for large scale preparations. It is highly probable that this approach can be extended as a general synthetic method for other metal sulfides such as PbS, Cu_2S, ZnS, WS_2, etc. A controlled aspect ratio and an enhanced yield can be obtained by suitably manipulating the growth conditions such as the composition of the reaction solvent, the amount of the precursor and the reaction temperature. Photoluminescence measurements at room temperature show that the synthesized CdS nanorods emit a strong and stable bluish green light and their luminescent peaks are at about 533 nm and 668 nm. Particle sizes calculated from the XRD and TEM images are found to be in good agreement. An unusual dendritic surface morphology was observed in the as-prepared sample. An optimum loading of 0.2 wt% of Pt/CdS was used to get maximum photocatalytic H_2 production.

Acknowledgment

We thank the Council for Scientific and Industrial Research (CSIR), New Delhi, India for research fellowship to one of the authors, CMJ.

References

[1] Peng X, Manna L, Yang L, Wickham J, Scher E, Kadavanich A and Alicisatos A P 2000 *Nature* **59** 404
[2] Li L, Walda J, Manna L and Alivisatos A P 2002 *Nano Lett.* **2** 557
[3] Cheon J, Kang N J, Lee S M, Lee J H, Yoon J H and Oh S J 2004 *J. Am. Chem. Soc.* **126** 1950
[4] Arora M K, Sinha A S K and Upadhyay S N 1998 *Ind. Eng. Chem. Res.* **37** 1310
[5] Darwent J R and Porter G 1981 *J. Chem. Soc., Chem. Commun.* **4** 145
[6] Matsumura M, Sato Y and Tsubomura H 1983 *J. Phys. Chem.* **87** 3807
[7] Borrell L, Cervera-March S, Gimenez J and Simarro R A 1992 *Sol. Energy Mater. Sol. Cells* **25** 25
[8] De G C, Roy A M and Bhattacharya S S 1996 *Int. J. Hydrog. Energy* **2** 19
[9] Wolkenstein T 1960 *Adv. Catal.* **12** 189
[10] Arora M K, Sahu N, Upadhyay S N and Sinha A S K 1999 *Ind. Eng. Chem. Res.* **38** 2659
[11] Wu L, Yu J C and Fu X 2006 *J. Mol. Catal.* A **244** 25
[12] Wang S, Liu P, Wang X and Fu X 2005 *Langmuir* **21** 11969
[13] Shangguan W and Yoshida A 2002 *J. Phys. Chem.* B **106** 12227
[14] Deshmukh L P, Holikatli S G and Hankare P P 1994 *J. Phys. D: Appl. Phys.* **27** 1786
[15] Khanna P K and Subbarao V V V S 2004 *Mater. Lett.* **58** 2801
[16] Wu X C and Tao Y R 2002 *J. Cryst. Growth* **242** 309
[17] Tian Y, Newton T, Kotov N A, Guldi D M and Fendler J H 1996 *J. Phys. Chem.* **100** 21
[18] Arora M K, Sinha A S K and Upadhyay S N 1998 *Ind. Eng. Chem. Res.* **37** 1310
[19] Zhu H, Yao K, Wo Y, Wang N and Wang L 2004 *Semicond. Sci. Technol.* **19** 1020
[20] Klug H P and Leroy E A 1974 *X-Ray Diffraction Procedures* (New York: Wiley) p 656
[21] Guo-yue X U and Wang H 2006 *Trans. Nonferrous Met. Soc.* **16** 105
[22] Tong H and Zhu Y J 2006 *Nanotechnology* **17** 845
[23] Tandon S P and Gupta J P 1970 *Phys. Status Solidi* **38** 363
[24] Lakowicz J R, Gryczynski I, Piszczek G and Murphy C J 2002 *J. Phys. Chem.* B **106** 5365
[25] Qin A M, Fang Y P, Zhao W X, Liu H Q and Su C Y 2005 *J. Cryst. Growth* **283** 230
[26] Subrahmanyam M, Supriya V T and Ramreddy P 1996 *Int. J. Hydrog. Energy* **21** 99
[27] Mau A W H *et al* 1984 *J. Am. Chem. Soc.* **106** 6537